# Tensile Elongation of High-Fluid Polypropylene/Ethylene–Propylene Rubber Blends: Dependence on Molecular Weight of the Components and Propylene Content of the Rubber

MASAHIRO NAIKI,[1] TAKENOBU MATSUMURA,[1] MASATOSHI MATSUDA[2]

[1] Ube Research Laboratory, Ube Industries, Ltd., 1978-96, Kogushi, Ube, Yamaguchi 755-8633, Japan

[2] Material Engineering Division II, Toyota Motor Corporation, 1, Toyota-cho, Toyota, Aichi 471-8572, Japan

*Received 16 May 2000; accepted 17 April 2001*

**ABSTRACT:** We studied tensile behavior of low-molecular-weight (MW) polypropylene (PP)/ethylene–propylene rubber (EPR; 70/30) blends from the viewpoint of the MWs of PP and EPR and the compatibility between PP and EPR. The value of the melt flow rate of PP varied from 30 to 700 g/10 min at 230°C. We studied the compatibility between PP and EPR by varying the propylene content in EPR (27 and 68 wt %). At the initial elongation stage, crazes were observed in all blends. When blends included EPR with 27 wt % propylene, the elongation at break of the low-MW PP improved little. The blends with EPR and 68 wt % propylene content were elongated further beyond their yielding points. The elongation to rupture was increased with increasing MW of EPR. Molecular orientation of the low-MW PP was manifested by IR dichroism measurements and X-ray diffraction patterns. The blends of low-MW PP and EPR could be elongated by the partial dissolution of EPR of high-MW in the PP amorphous phase.
 J Appl Polym Sci 83: 46–56, 2002

**Key words:** low-molecular-weight poly(propylene) (PP); ethylene–propylene rubber; compatibility; elongation; morphology

## INTRODUCTION

Polypropylene (PP) is often blended with rubbers of low modulus and low glass-transition temperature ($T_g$) to improve its impact strength at low temperatures.[1] As the rubber component, various ethylene-$\alpha$-olefin copolymers, styrenic elastomers, and related compounds are used.[2] The rubbers usually form dispersed particles, and the mechanical properties of the blends greatly depend on the size of the rubber particle and the interfacial adhesion between the components.[3,4] The size of the rubber particle is usually determined by the viscosity ratio of the matrix PP and the dispersed rubber in addition to the compatibility between them.[5,6] In other words, physical properties of PP/rubber blends can be widely varied by the proper combination of PP and rubber.

The study of the deformation of PP/rubber blends, especially those of PP/ethylene–propylene rubber (EPR) blends, has focused on various characteristics,[1] including rubber particle size,[3] crystallization and deformation temperature,[7] matrix crystallinity,[8] and compatibility of PP and rubber.[9–12] The PP samples used in these studies had, in most cases, molecular weights (MWs) higher than several hundreds of thousand and were ductile without adding rubber.

*Correspondence to:* M. Naiki.

In polymer processing, such as the injection molding of large parts such as automobile bumpers, high fluidity of the melts is favored. Although the fluidity of the blends can be improved by a simple decrease in the MW of the components, lowering the MW usually leads to a decrease in toughness. Therefore, it is necessary to know the lowest MW that is usable for the matrix polymer.

On the deformation of PP/rubber blends, the effect of the MW of PP has been discussed little. Notably, the tensile deformation of low-MW PP toughened by rubber was studied by Nomura and colleagues only.[13–15] They showed that the addition of EPR of more than 30 wt % is one of the requirements for the manufacture of ductile low-MW PP. However, the effect of the rubber on the elongation and the mechanism of the deformation have not been clarified sufficiently.

In this report, we focus our attention to the tensile deformation of the blends of low-MW PP and EPR. We investigated the effect of the MW of PP and EPR and the compatibility between them on the elongation of the blends. The MW of PP used in this study was much lower than that of previous works.[3,7–12] We discuss the requirement of EPR for the manufacture of ductile low-MW PP and clarify the mechanism of elongation of the of low-MW PP and EPR.

## EXPERIMENTAL

### Materials

PPs used in this study were supplied by Grand Polymer Co., Ltd., Chiba, Japan. The melt flow rates (MFRs) lay between 30 and 700 g/10 min at 230°C (ASTM D1238). Four kinds of EPR were used; one had a propylene content of 26 wt %, and the others with different MWs had a propylene content of 68 wt %. The molecular characteristics of PP and EPR are summarized in Tables I and II, respectively.

**Table I Characteristics of PP Samples**

| PP | MFR[a] (g/10 min at 230°C) | $M_W$[b] | $M_W/M_n$[b] | mmmm[c] |
|---|---|---|---|---|
| PP1 | 31 | 300,000 | 6.8 | 0.979 |
| PP2 | 170 | 150,000 | 6.8 | 0.985 |
| PP3 | 250 | 120,000 | 5.5 | 0.985 |
| PP4 | 400 | 110,000 | 6.9 | 0.985 |
| PP5 | 700 | 89,000 | 5.9 | 0.985 |

$M_n$ = number-average molecular weight.
$M_W$ = weight-average molecular weight.
mmmm = isotactic pentad fraction of four successive meso dyad.
[a] ASTM D1238.
[b] Determined by gel-permeation chromatography.
[c] Determined by $^{13}$C-NMR.

**Table II Characteristics of EPR Samples**

| EPR | Propylene Content (wt %) | $M_W$ | $M_W/M_n$ | MFR[a] (g/10 min at 230°C) |
|---|---|---|---|---|
| EPR1 | 68 | 148,000 | 3.2 | 11 |
| EPR2 | 68 | 320,000 | 7.0 | 2.4 |
| EPR3 | 68 | 470,000 | 6.4 | 0.4 |
| EPR4 | 26 | 200,000 | 3.8 | 3.0 |

[a] ASTM D1238.

The PP and EPR were blended in a twin-screw Brabender-type plasticorder (Katotech, Kyoto, Japan) with a blending time of 5 min at 230°C and 60 rpm. The blend composition was PP/EPR = 70/30(wt/wt). After blending, the materials were remelted and pressed into sheets 1 mm and 50 $\mu$m thick at 230°C for 5 min and cooled at 30°C. The sheets were punched into dumbbell- and rectangular-shaped bars.

### Measurements

Dynamic mechanical analysis was performed with a Rheometoric Scientific (Piscataway, NJ) RSA-II in tension-compression mode from −100°C to melting at a frequency of 10 Hz and a strain of 0.05%. Temperature dependence of the storage modulus ($E'$) and the loss modulus ($E''$) of the blends and the component polymers was measured.

Thermal properties were studied by a differential scanning calorimeter (PerkinElmer DSC7; Norwalk, CT); the heating and cooling rate was 10°C/min. The temperature and the heat of fusion were calibrated by indium as a standard. Crystallinity was determined from the endothermic area of the second heating run with the value of $\Delta h^0$ = 209 J/g for PP.[16]

The stress–strain behavior of dumbbell-shaped bars 1 mm thick was measured at 23°C at a crosshead speed of 5 mm/min with an Orientec (Tokyo, Japan) Tensiron UCT-5T testing machine. The strain was taken as the ratio of the increment of the distance between clumps to the initial one.

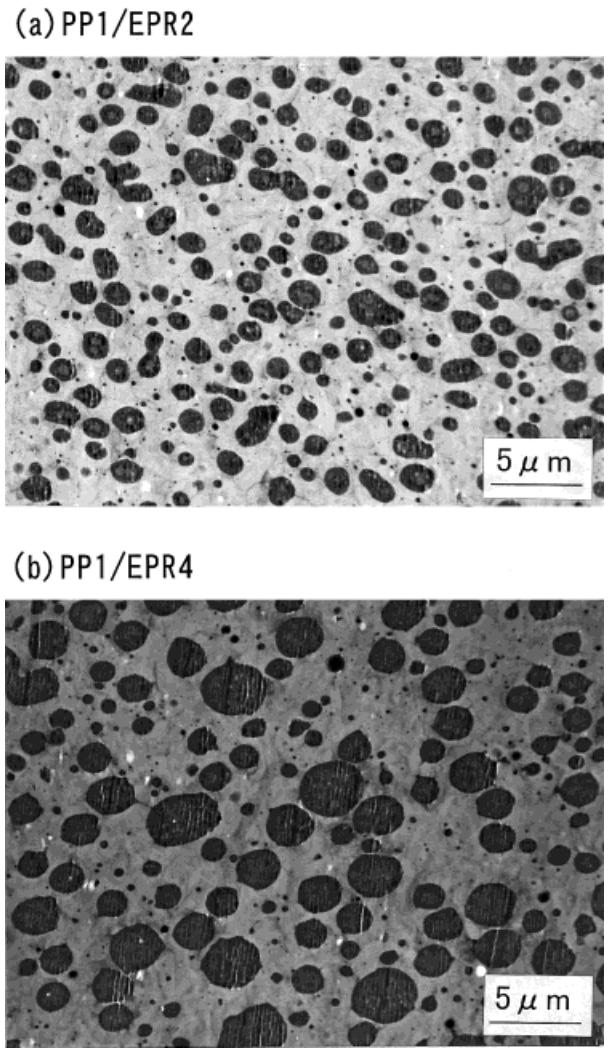


**Figure 1** Morphologies of the blends of PP1 and EPR: (a) PP1/EPR2 and (b) PP1/EPR4.

The rupture surfaces after the stress–strain measurements were investigated without any modification by means of a Laser Tech (Kanagawa, Japan) 1LM15 scanning laser microscope (SLM).

Observation of the morphology before and after deformation of PP/EPR blends was carried out by a JEOL (Tokyo, Japan) JEM-200CX transmission electron microscope (TEM). The crazes were observed on the 50 $\mu$m thick rectangular specimens elongated up to their yielding points. The samples to be analyzed were stained with ruthenium tetroxide for 2 and 1.5 h for PP/EPR2 and PP/EPR4 blends, respectively, and sectioned with an ultramicrotome. Ultrathin sections 100 nm thick were observed.

The surface at several strain stages was studied with a Hitachi (Tokyo, Japan) S-2150 scanning electron microscope (SEM). The 50 $\mu$m thick rectangular specimens were elongated to the desired strain, where the strain was fixed by placement of the specimens between two metal plates. The surfaces of the specimens were etched by ultrasonic radiation in xylene at room tempera-

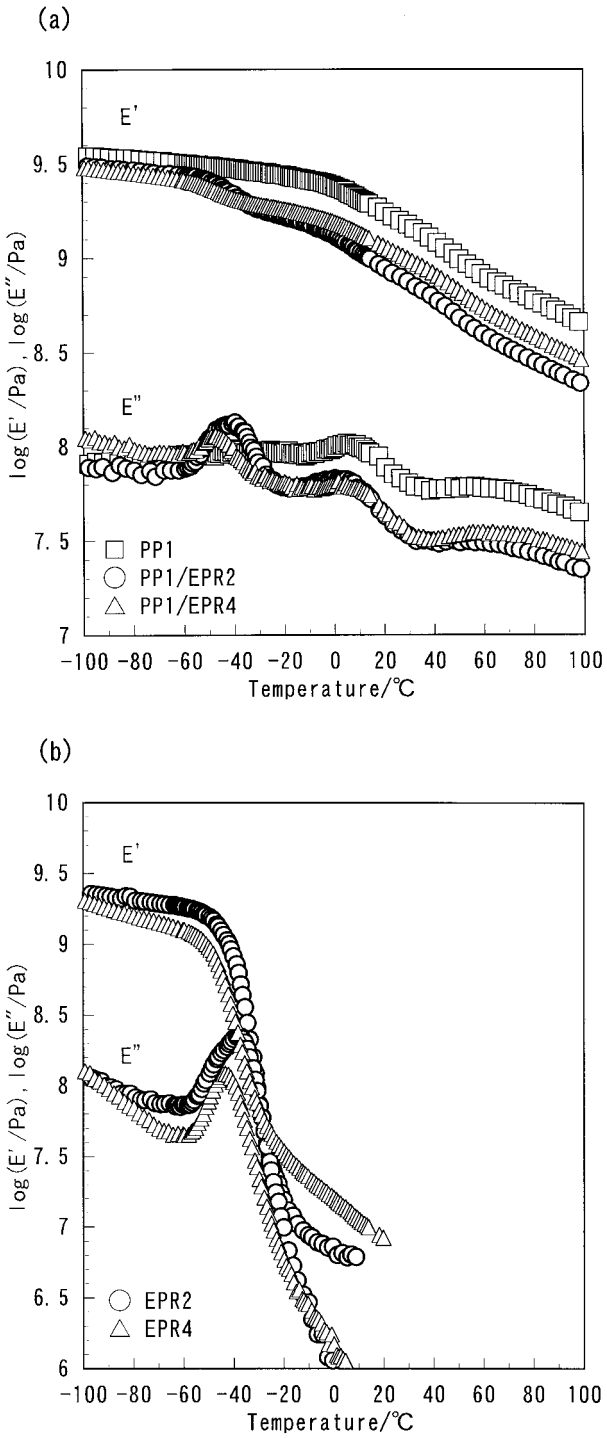


**Figure 2** Temperature dependence of E′ and E″ for (a) PP1 and PP1/EPR blends and (b) EPR.

**Table III Weight Fraction of EPR in the PP Amorphous Phase**

| | Weight Fraction | | | |
|---|---|---|---|---|
| | EPR1 | EPR2 | EPR3 | EPR4 |
| PP1/EPR | — | 0.091 | — | 0.025 |
| PP2/EPR | 0.22 | 0.086 | 0.063 | 0.023 |
| PP3/EPR | — | 0.084 | — | 0.023 |

ture and coated with gold, and they were observed with the strain fixed.

The orientation of the molecular chain by elongation was evaluated from the orientation function, which was determined by the IR dichroism measurement.[17] Polarized IR spectra were measured by a PerkinElmer 1750 Fourier transform IR spectrometer. The 50 $\mu$m thick sample elongated to a specified strain state was fixed by a sample holder. IR spectra from the center of the elongated region were measured. When the axis of a molecular chain makes an angle ($\theta$) to a drawing direction and a transition dipole moment makes an angle ($\beta$) to the molecular axis, the orientation function ($f$) is given by the following equation:

$$f = \frac{3(\cos^2\theta) - 1}{2} = \frac{1 - D}{c(1 + 2D)} \quad (1)$$

where $D$ is the dichroic ratio, $D = A_{\perp}/A_{\parallel}$, and

$$c = \frac{3\ \cos^2\beta - 1}{2} \quad (2)$$

We measured the absorbance at 998, 973, and 722 $cm^{-1}$, which are assigned to the crystalline PP, amorphous PP, and ethylene sequence in EPR, respectively.[18–20]

Wide angle X-ray diffraction studies were carried out with a Mac Science (Kanagawa, Japan) DIP220 X-ray diffractometor equipped with an imaging plate. The graphite monochromatized X-ray (40 kV, 250 mA) was transmitted perpendicular to the drawing axis of the sample.

## RESULTS AND DISCUSSION

### Morphology

TEM photographs of the PP1/EPR2 and PP1/EPR4 blends are shown in Figure 1, where the heterogeneity of the blends is displayed. EPR appears as dispersed dark particles in these images. The size of the dispersed phase in PP1/EPR2 blend was smaller than that in PP1/EPR4. The viscosity ratio of the components in polymer blends is known to be an influential parameter for determining the morphologies;[5] as the viscosities of the components approach each other, the particle size of the blend becomes smaller. According to this criterion, because the MFR value of EPR2 was smaller than that of EPR4, the size of the dispersed particles in PP1/EPR2 blend may have been larger than that in PP1/EPR4. In practice, however, the opposite tendency was observed. Therefore, in this instance, the propylene content in EPR determined the size of the dispersed particles of the PP/EPR blends. The other blends were also heterogeneous like the PP1/EPR blends.

### Dynamic Mechanical Analysis

The temperature dependence of $E'$ and $E''$ of PP1/EPR2 and PP1/EPR4 blends and their components is shown in Figure 2. Interpretation of the dynamic mechanical analysis of the PP/EPR blends has been well described.[12,21] The decreases in $E'$ at about $-40$ and 10°C were attributed to the glass transitions of EPR and PP, respectively. The appearance of the glass transition of each component in the blends indicates that these blends were phase-separated systems. This corresponds with Figure 1.

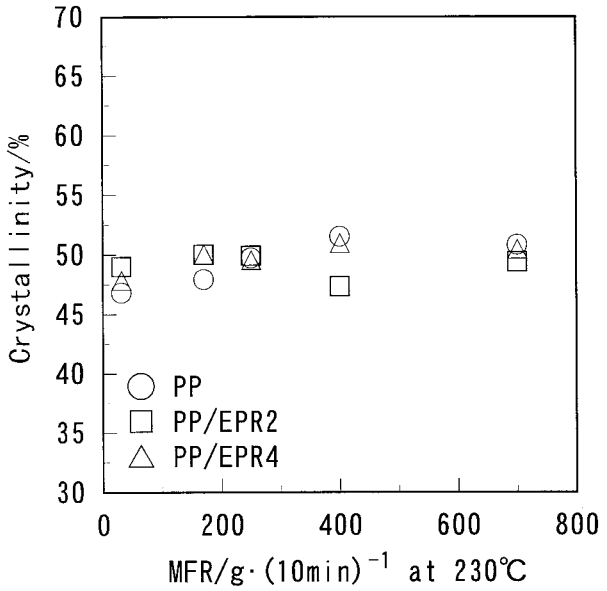


**Figure 3** Crystallinity of (○) PP, (□) PP/EPR2, and (△) PP/EPR4 as a function of PP MFR.

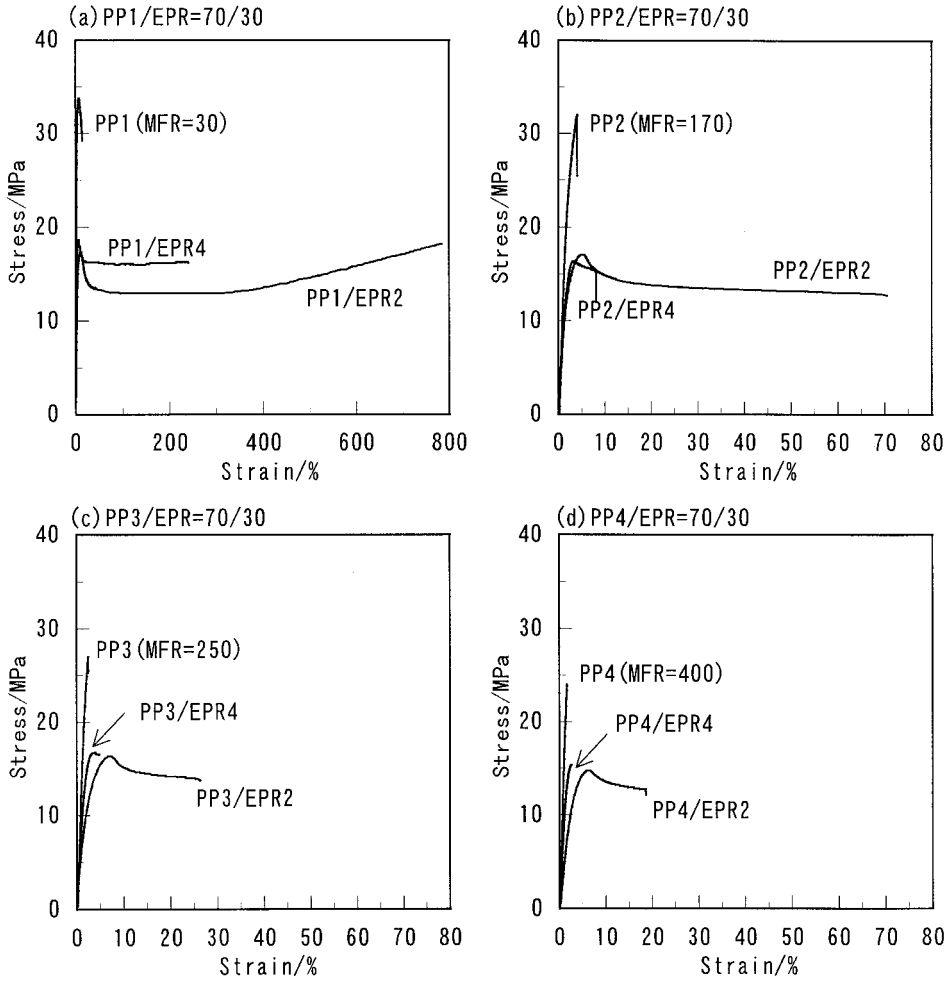


**Figure 4** Stress–strain curves for PP and PP/EPR blends at 23°C.

$T_g$ of the EPR component in the PP1/EPR blends was almost equal to that of EPR alone. However, $T_g$ of the PP component of the blends near 10°C shifted to lower temperatures by a few degrees. EPR2 could shift $T_g$ of the PP component to a lower value than EPR4. This lowering of $T_g$ arose from the partial dissolution of the EPR components in the PP amorphous phase. From the shift of $T_g$, it is possible to estimate the concentration of EPR in the PP amorphous phase with Fox's equation:[22]

$$\frac{1}{T_{gb}} = \frac{w_1}{T_{g1}} + \frac{w_2}{T_{g2}} \tag{3}$$

where $T_{gb}$, $T_{g1}$, and $T_{g2}$ are $T_g$'s of the PP components in PP/EPR blends, PP, and EPR, respectively, and $w_1$ and $w_2$ are the weight fractions of PP and EPR in the PP amorphous phase, respectively. The weight fractions of EPR in the PP amorphous phase are shown in Table III. The quantities of the dissolved EPR in PP/EPR2 blends were larger than those in PP/EPR4. EPR2 had a higher compatibility with PP, and the particle size in PP/EPR2 blends was smaller, as shown in Figure 1. The dissolved EPR in the PP2/EPR blends decreased as the MW of EPR increased.

### Crystallinity

It is clear that the mechanical properties of a crystalline polymer greatly change with its crystallinity. The crystallinity of PP and PP/EPR blends, determined from thermal analysis, is plotted in Figure 3 as a function of the MFR of PP. The crystallinity slightly increased with increasing MFR of PP; PP crystallized more easily as the MW became smaller.

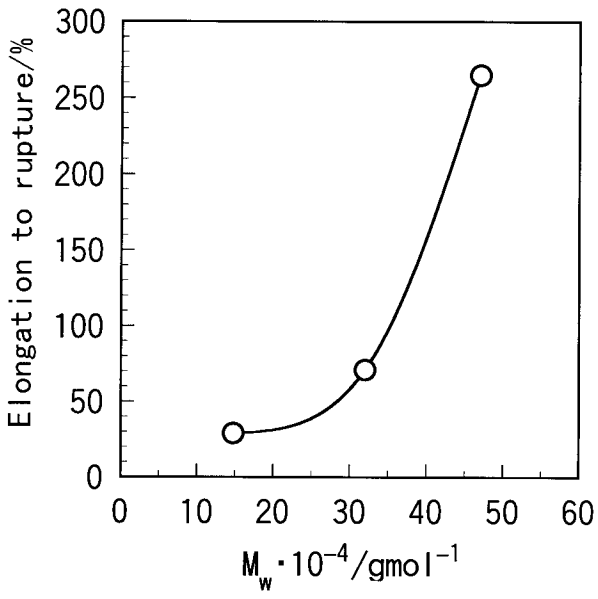


**Figure 5** Elongation to rupture of PP2/EPR blends as a function of the MW of EPR. Propylene content of EPR = 68 wt %.

### Stress–Strain Behavior

Stress–strain curves of PP and PP/EPR2 and PP/EPR4 blends are shown in Figure 4. The Young's moduli were lowered by the addition of EPR to PP. The elongation to rupture generally increased with increasing MW of PP and by addition of EPR. In the case of PP2, PP3, and PP4, EPR4 increased the elongation to rupture only a little; whereas EPR2 enabled much larger elongation further beyond their yielding points. Thus, the ductility of the low-MW PP was found to be greatly changed by blending with EPR2. This agrees well with Nomura and coworker's data that the elongation to rupture of a low-MW PP with an intrinsic viscosity of 0.89 dL/g greatly increased when blended with EPR with propylene content of 62 wt %.[13]

The blends of EPR with PP5 with the lowest MW were found to break before their yielding points, and the mechanical properties could not be improved by the addition of EPR.

The difference in the crystallinity of various PP/EPR blends was only within 2% (Fig. 3), and this was too small to induce such a large difference in the elongation. The elongation to rupture was thus determined by the compatibility of EPR with PP.

Figure 5 shows the elongation to rupture of the blends of PP2 and EPR2-type rubber with varied MWs. The elongation to rupture increased with increasing MW of EPR. This indicates that EPR with a higher MW is preferable for the manufacture of ductile low-MW PP.

### Morphology of Elongated Samples

The morphology of the samples after deformation was observed by SLM, TEM, and SEM to examine why the elongation at break of the PP/EPR blends greatly changed with the propylene content of EPR.

Figure 6 shows the SLM photographs of the surface in the rupture area after tensile measurement of PP/EPR blends. The change in the morphology is displayed as functions of the MW of PP and compatibility of EPR. The number of crazes increased with increasing MW of PP. The PP/EPR2 blends that were elongated beyond their yielding points had much more abundant crazing than the PP/EPR4 blends that broke at or just after their yielding points. Dense crazing was found necessary for the elongation of PP/EPR blends beyond the yielding point.

Detailed observations in the initial stages of elongation were also carried out with a TEM. Figure 7 shows the TEM photographs of the PP2/EPR2 and PP2/EPR4 blends elongated up to the yielding points. In both samples, crazes grew by the rubber particles perpendicular to the stretching direction. This shows that they were deformed, relieving the concentrated stress by crazing; we could not find any shear yielding bands. The crazes formed in the initial deformation were quite different from each other; the small crazes grew by the small rubber particles in the PP2/EPR2 blend, whereas the large crazes grew by the large rubber particles in PP2/EPR4. Donald and Kramer[23] demonstrated in high-impact polystyrene that the stress around a rubber particle decreased with the distance from the rubber particle; the stress became half at a position one-tenth of a particle size away. That is to say, the larger crazes grew by the larger particles because the stress concentration zone around them was larger.

From the SLM and TEM observations, the elongation of the PP2/EPR2 blend was attended with successive crazes. On the other hand, the PP2/EPR4 blend was broken near the yielding point because the large crazes easily grew to cracks.

Margolina and Wu[24] demonstrated that polymer blends become ductile when the interparticle distance is smaller than a threshold value. The interparticle distance of the PP/EPR2 blend was

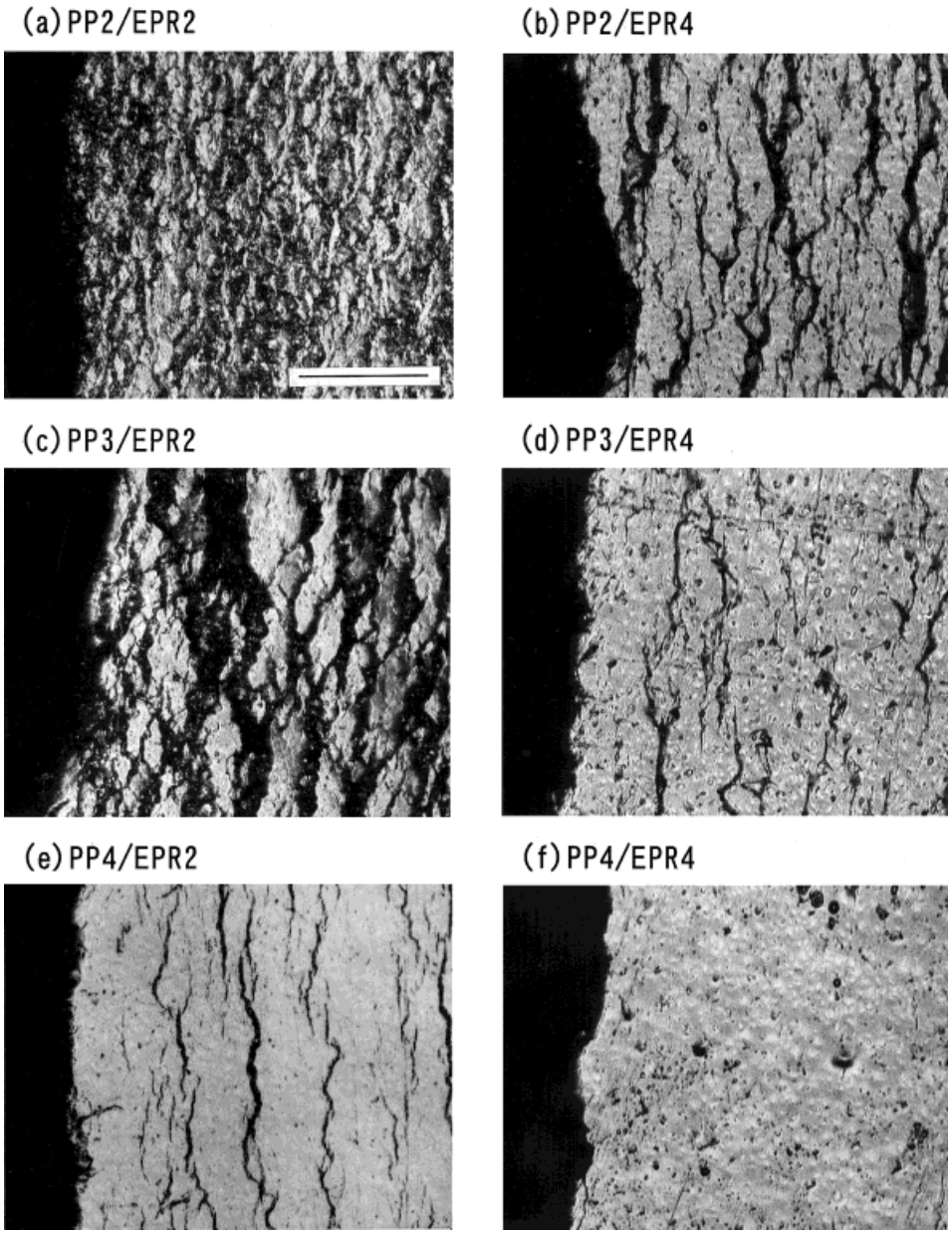


**Figure 6** SLM micrographs of PP/EPR blends of fracture surfaces: (a) PP2/EPR2, (b) PP2/EPR4, (c) PP3/EPR2, (d) PP3/EPR4, (e) PP4/EPR2, and (f) PP4/EPR4. Scale bar = 100 $\mu$m.

smaller than that of PP/EPR4, and the elongation to rupture was considered to be correlated with the interparticle distance.

The morphology of the PP2/EPR2 blend after yielding points was observed by SEM, where the rubber particles at the surface were removed by ultrasonic radiation in xylene. Figure 8(a) shows the photograph immediately after the yielding point. Crazes grew both in width and in length. Figure 8(b,c) shows the morphology for 25 and 50% tensile elongation, where the clear fibrilar structure developed with an increase in strain and the undeformed regions remained at the both ends of the fibrilar structure. As shown in a series of SEM photographs, the elongation seemed to occur through craze elongating; the crazes extended in length and in width, making the undeformed matrix form fibrilar morphology. After the yielding point, the necking region consisted of the fibrous regions and the undeformed regions.

The SEM photograph of PP2/EPR4 blend just after the yielding point is shown in Figure 9.

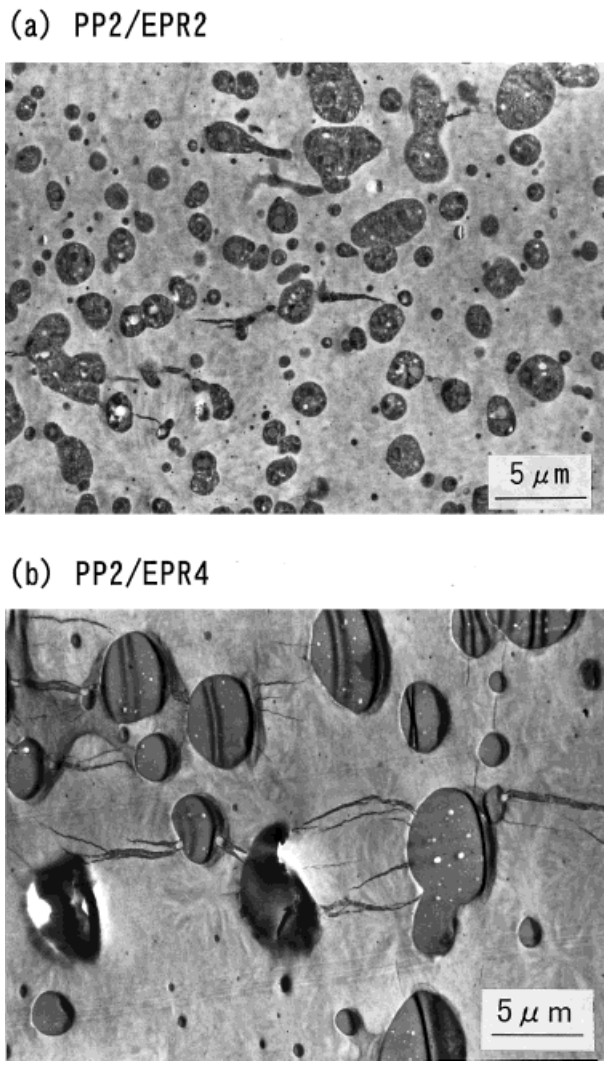


**Figure 7** TEM photographs of PP2/EPR blends elongated near the yielding point showing crazes from the rubber particles: (a) PP2/EPR2 and (b) PP2/EPR4.

Fibrilar morphology was not observed. Whether fibrilar morphology was developed depended on the propylene content of EPR in the blends. The boundaries between the craze and undeformed matrix of PP2/EPR4 blend clearly differed from those of PP2/EPR2 shown in Figure 8(a); those in the former appeared distinct, whereas those in the latter were blurred. The difference between the brittle and ductile materials was clearly shown by the shape of the crazes.

### IR Dichroism Measurements

A rheo-optical technique such as IR dichroism measurement is very useful for interpretation of the deformation process of crystalline polymers.[9,25–27] We evaluated the orientation of the molecular chain in the tensile deformation process by IR dichroism measurements. This method is useful for the independent estimation of the

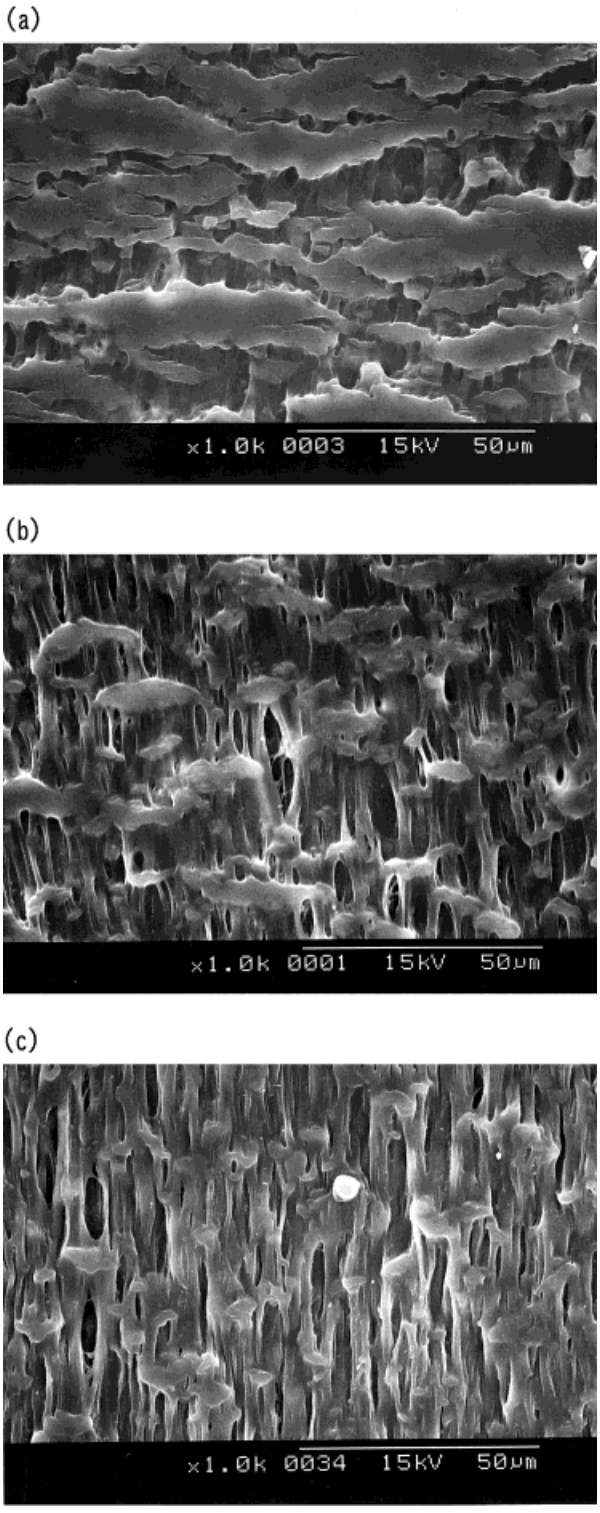


**Figure 8** SEM micrographs of the elongated PP2/EPR2 blend: (a) just after the yielding point, (b) at tensile strain = 25%, and (c) at tensile strain = 50%.

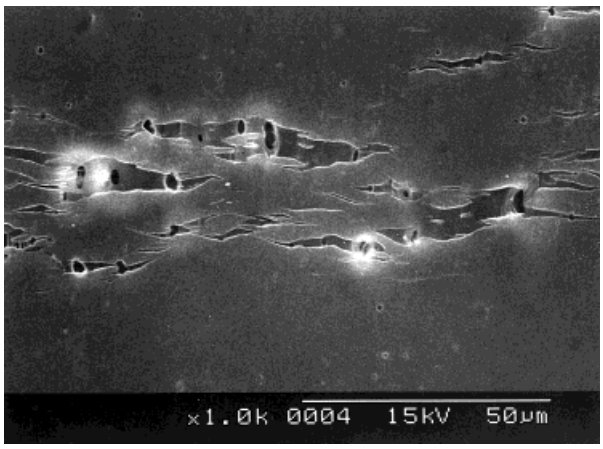


**Figure 9** SEM micrographs of the PP2/EPR 4 blend elongated just after the yielding point.

orientations of the PP crystal phase, PP amorphous phase, and rubber.

Figure 10 shows the strain dependence of the orientation functions for the PP2/EPR2 blend compared with its stress–strain curve. The orientation functions of the PP crystal phase, PP amorphous phase, and rubber up to the yielding point had a slightly negative value or zero. After the yielding point, the orientation functions of PP increased with an increase in strain. Such change of the orientation function is similar to the results of blends of high-MW PP and EPR by Onogi et al.[27] Even in the blend of low-MW PP and EPR, the PP chains were oriented by tensile elongation

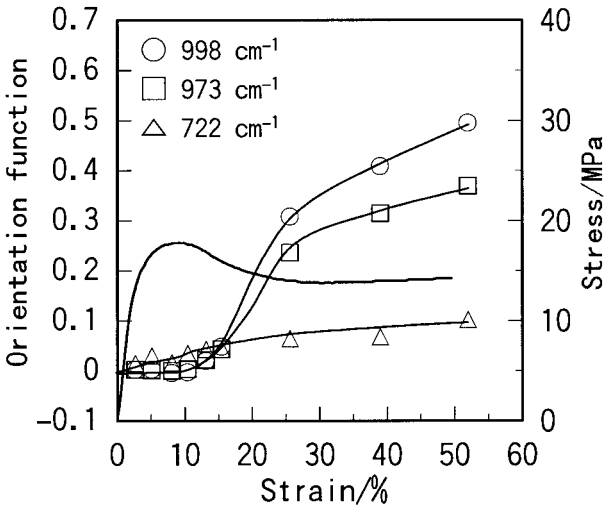


**Figure 10** Strain dependence of the orientation functions for the bands at 998 $cm^{-1}$ (PP crystalline phase), 973 $cm^{-1}$ (PP amorphous phase), and 722 $cm^{-1}$ (EPR) of the PP2/EPR2 blend.

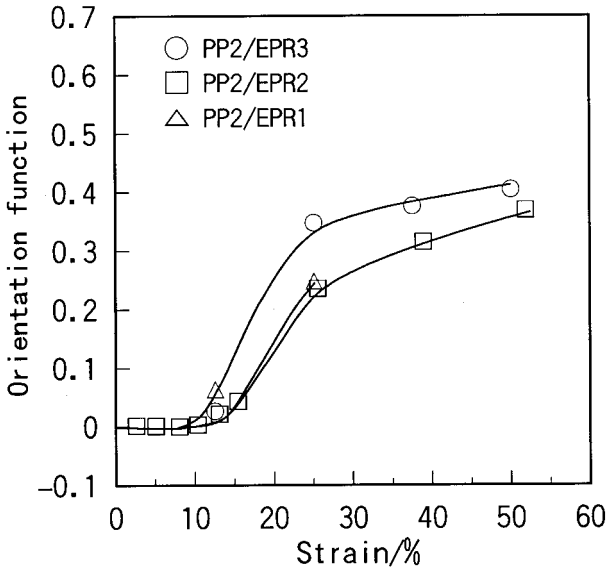


**Figure 11** Strain and EPR molecular-weight dependence of the orientation functions for the PP amorphous phase (973 $cm^{-1}$). Propylene content of EPR = 68 wt %.

in a similar manner as in blends of high-MW PP and EPR.

The dependence of the orientation function of the PP amorphous phase on the MW of EPR is shown in Figure 11. The propylene content of EPR used was 68 wt %. The orientation function of the PP2/EPR3 blends was largest among three blends. This was due to the larger number of chain entanglements in the PP amorphous phase in which EPR of higher MW dissolves.

### X-Ray Diffraction Patterns

We qualitatively examined the crystalline structure and orientation in elongating the PP2/EPR2 blend by two-dimensional X-ray diffraction patterns. Figure 12 shows the X-ray patterns for 0, 25, and 50% tensile elongation. Before elongation, the Debey–Scherrer rings, which confirmed the unoriented structure of the $\alpha$-phase, were observed. When the sample was elongated, diffuse diffraction increased on the equator and in the diagonal direction with an increase in strain. This was due to the orientated smectic phase, not the $\alpha$ crystal.[28] The diffraction pattern for 50% strain was similar to Fig.6 in Ref. 28, which was taken for the PP/EPR (80/20) blend whose MW of PP was $3.07 \times 10^5$. The PP2/EPR2 blend deformed in a similar manner as the blends of conventional higher MW PP and EPR.

The isotropic rings were still visible in the diffraction patterns after deformation. This agrees

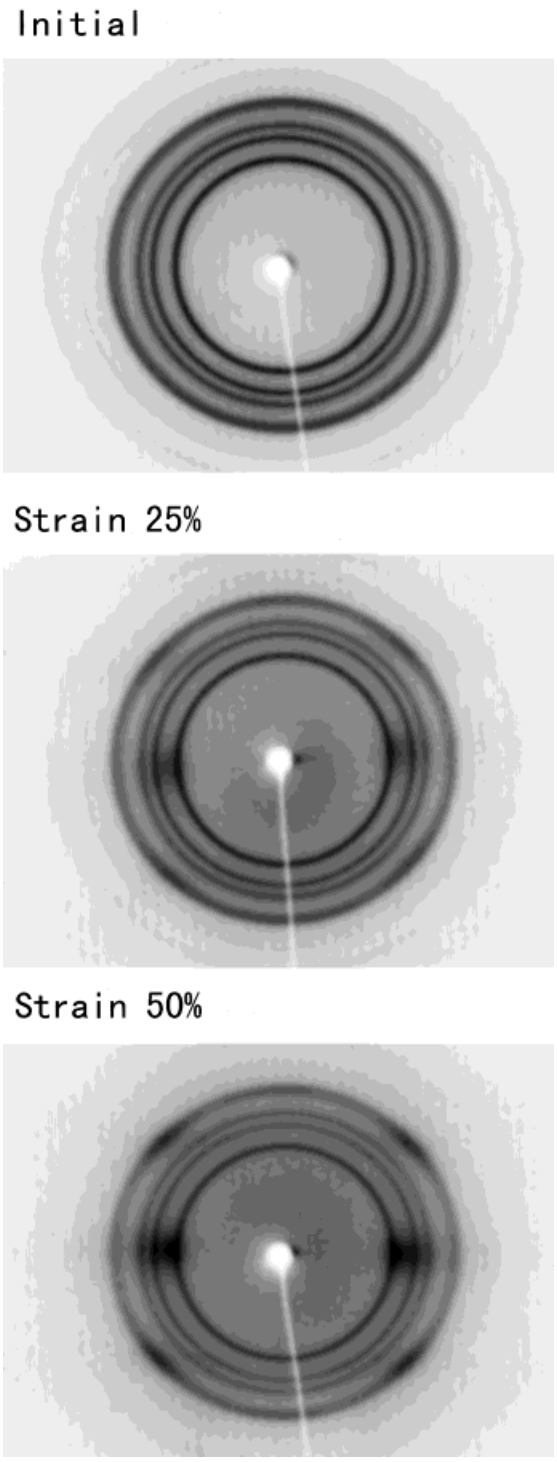


**Figure 12** X-ray diffraction patterns of the PP2/EPR2 blend drawn up to 0, 25, and 50% strain.

with the SEM photographs of the deformed sample shown in Figure 8(b,c), where we observed the oriented and the undeformed region.

The smectic phase had the crystalline band in the IR spectrum at 998 $cm^{-1}$.[29] Therefore, the orientation of the smectic phase was found to be measured as that of the PP crystalline phase in the IR dichroism measurements.

### Requirement for Elongation of Low-MW PP/EPR Blends

Regardless of the propylene content of EPR, the blends of low-MW PP and EPR were elongated with generating crazes. The size of crazes was determined by the morphology, such as the size of dispersed particles, of the polymer blends. Therefore, EPR should be finely dispersed to avoid the formation of large crazes, which easily grow to fatal cracks.

The PP2/EPR2 and PP2/EPR3 blends could be elongated beyond the yielding point, and the quantity of deformation was larger than the sum of the crazes. EPR of 68 wt % propylene content were partially dissolved in the PP amorphous phase, and the elongation to rupture increased with increasing MW of EPR. Therefore, EPR dissolved in the PP amorphous phase plays an important role in the elongation of low-MW PP.

The MWs of EPR2 and EPR3 dissolved in the PP amorphous phase were much higher than that of PP2. The polymer chains of PP and EPR2 or EPR3 in the PP amorphous phase had higher degrees of entanglement. Consequently, the low-MW PP could deform as if it had a higher MW. In addition, the fibrilar morphology shown by the SEM photographs implies that not only the PP amorphous phase but also the PP crystalline phase deformed. This was confirmed by X-ray diffraction and IR dichroism measurements. The PP chains in the amorphous phase including dissolved EPR could transmit the stress to the crystal without a rupture.

Coppola et al.[7] showed that the ductility of PP/EPR blends increased with decreasing crystallization temperature. They explained the difference in the ductility based on the number of tie molecules in the samples crystallized at different temperatures. In our system of the low-MW PP, the entanglements of PP and dissolved EPR carried load and contributed to breaking lamellae. According to the dependence of the orientation function of the PP amorphous phase on the MW of EPR (Fig. 11), the number of entanglements in the PP amorphous phase was considered to increase with increasing MW of the dissolved EPR. This would be responsible for the increase in the elongation to rupture with increasing the MW of EPR. The EPR dissolved in the PP amorphous phase should have had higher MW for elongation of the blends of low-MW PP.

## CONCLUSIONS

We examined the elongation of the blends of low-MW PP and EPR and elucidated the requirement of EPR for elongating the low-MW PP.

When EPR with a larger propylene content and a larger compatibility with PP was added to the low-MW PP with a MFR of 170–400 g/10 min, the blends could be elongated over their yielding points. The elongation occurred through craze elongation both in length and in width, and fibrilar morphology was formed, which indicates that the matrix PP, not only the amorphous phase but also the crystalline phase, deformed. The elongation to rupture increased with increasing the MW of EPR. EPR dissolved in the PP amorphous phase greatly affected the deformation of the PP matrix. The chain entanglements between PP and high-MW EPR in the PP amorphous phase could transmit a load to deform PP lamellae. The following necessary conditions for the elongation of the blends of low-MW PP and EPR were found: that EPR partially dissolved in the PP amorphous phase and that the MW of the dissolved EPR was higher.

The authors are particularly indebted to Professor T. Yamamoto of Yamaguchi University for his help in the preparation of this article. The authors also thank T. Akagawa of Grand Polymer Co., Ltd., for kindly supplying PP samples.

## REFERENCES

1. Martuscelli, E. In Polypropylene: Structure, Blends and Composites; Karger-Kocsis, J., Ed.; Chapman & Hall: London, 1995; Vol. 2, Chapter 4.
2. Utracki, L. A. In Polypropylene: An A–Z Reference; Karger-Kocsis, J., Ed.; Kluwer Academic: London, 1999; p 621.
3. Jang, B. Z.; Uhlmann, D. R.; Sande, J. B. V. Polym Eng Sci 1985, 25, 643.
4. Wu, S. Polymer 1985, 26, 1855.
5. Wu, S. Polym Eng Sci 1987, 27, 335.
6. Nomura, T.; Nishio, T.; Maeda, S.; Kamei, E. Nippon Reoroji Gakkaishi 1994, 22, 155.
7. Coppola, F.; Greco, R.; Martuscelli, E.; Kammer, H. W.; Kummerlowe, C. Polymer 1987, 28, 47.
8. Van der Wal, A.; Mulder, J. J.; Oderkerk, J.; Gaymans, R. J. Polymer 1998, 39, 6781.
9. Nitta, K.; Okamoto, K.; Yamaguchi, M. Polymer 1998, 39, 53.
10. Greco, R.; Mancarella, C.; Martuscelli, E.; Ragosta, G.; Jinghua, Y. Polymer 1987, 28, 1929.
11. D'Orazio, L.; Mancarella, C.; Martuscelli, E.; Cecchin, G.; Corrieri, R. Polymer 1999, 40, 2745.
12. Yamaguchi, M.; Miyata, H.; Nitta, K. J Appl Polym Sci 1996, 62, 87.
13. Nomura, T.; Nishio, T.; Fujii, T.; Sakai, J.; Yamamoto, M.; Uemura, A.; Kakugo, M. Polym Eng Sci 1995, 35, 1261.
14. Nomura, T.; Nishio, T.; Sato, H.; Sano, H. Kobunshi Ronbunshu 1993, 50, 19.
15. Nomura, T.; Nishio, T.; Sato, H.; Sano, H. Kobunshi Ronbunshu 1993, 50, 81.
16. Van Krevelen, D. W. In Properties of Polymers, 3rd ed.; Elsevier Science: Amsterdam, 1990; Chapter 5.
17. Zbinden, R. In Infrared Spectroscopy of High Polymers; Academic: New York, 1964; 166.
18. Tadokoro, H.; Kobayashi, M.; Ukita, M.; Yasufuku, K.; Murahashi, S.; Torii, T. J Chem Phys 1965, 42, 1432.
19. Miyazawa, T. J Polym Sci Part C 1964, 7, 59.
20. Krimm, S.; Liang, C. Y.; Sutherland, G. B. B. M. J Chem Phys 1956, 25, 549.
21. Nomura, T.; Nishio, T.; Maeda, S.; Kamei, E. Nippon Reoroji Gakkaishi 1994, 22, 165.
22. Fox, T. G. Bull Am Phys Soc 1956, 1, 123.
23. Donald, A. M.; Kramer, E. J. J Appl Polym Sci 1982, 27, 3729.
24. Margolina, A.; Wu, S. Polymer 1988, 29, 2170.
25. Onogi, S.; Asada, T.; Hirai, M.; Kameyama, K. Zairyou 1965, 14, 322.
26. Onogi, S.; Asada, T.; Takagi, T. Zairyou 1967, 16, 746.
27. Onogi, S.; Asada, T.; Tanaka, A. J Polym Sci Part A-2 1969, 7, 171.
28. Kammer, H. W.; Kummerlowe, C.; Greco, R.; Mancarella, C.; Martuscelli, E. Polymer 1988, 29, 963.
29. Natta, G.; Peraldo, M.; Corradini, P. Atti Acc Naz Lincei 1959, 26, 14.